GROUND VIBRATION TEST USING ACOUSTIC EXCITATION: APPLICATION ON A COMPOSITE WING

Leonardo de Paula Silva Ferreira*, Lazaro Valentim Donadon*, Paulo Henriques Iscold Andrade de Oliveira*
***Federal University of Minas Gerais – Mechanical Engineering Department**

Keywords: *Ground vibration test, acoustic excitation, modal analysis*

Abstract

Ground vibration testing is essential for the accurate determination of the dynamic behavior of structural components, especially in aerospace industry. The information obtained from these tests helps the validation and improvement of dynamic models used in various stages of design. Among other functions, these models predict the natural frequencies and mode shapes of the structure. The most common methods for vibration test make use of an electromechanical shaker. This type of driver may cause problems both for the test as to the structure. This paper presents the application of a vibration test methodology using acoustic excitation. It aims at reducing the number of equipment needed to perform the test as well to obtain a form of excitation less intrusive to the structure. The test was performed in a composite wing with known numerical frequencies. Its fundamental frequencies and mode shapes obtained from analytical and numerical way were compared with experimental results and showed good results. In addition, several factors that influence the results of modal analyzes, such as noise effects, frequency response function (FRF) estimators and data processing, are evaluated.

1 Introduction

An aircraft wing is an elastic structure and in presence of aerodynamic loads, it starts to vibrate. Because of self-excitation, the natural frequencies change during flight. If the changes of natural frequencies occur in a direction in which the magnitude of the bending and torsional frequencies of the wing are the same, the aircraft will experience a catastrophic phenomenon called flutter [1]. The design of an aircraft must avoid it. One way to predict the occurrence of it is the use of dynamic models of the aircraft. These models use, among others information, the aircraft vibrational behavior. The natural frequencies and modal shapes can be obtained by several ways, including finite elements analysis and modal experiments, known as Ground Vibration Testing (GVT).

GVT of aircraft is typically performed very late in the development test. The main objective of a GVT is to determine experimentally the low-frequencies modes of the aircraft for validating and improving its dynamic model. More complex aircraft design and the usage of composite materials raised additional testing requirements. At the same time, there is only a short period in which the fully assembled aircraft is available for testing, due to limited schedule and high cost of down time [2]. This scenario has motivated a lot of international research.

A typical laboratory vibration test often involves a single force applied in one direction by a high impedance electrodynamic shaker [3]. In contrast, when in flight, an aerial vehicle is excited over its external surface by normal and tangential fluid forces in all directions. It should be noted that attach the structure to the shaker significantly alters its dynamics response. Moreover, some structures are very fragile and can be damaged during the experimental testing.

One solution for the excitation problem is use a pressure wave to excite the aircraft. It would avoid problems with contact and can excite the whole structure [4]. Acoustic excitation is used for many purposes, including

damage detection [5], load simulation [6], fluid flow [7] and many others.

Several configurations are possible, but the simplest is an amplifier and a speaker sending known waves to the structure. Moreover, the test can be faster than the traditional ones, since the initial setup is easier. The operator just need to select the wave, turn on the speaker and move a sensor through the structure, e.g., an accelerometer or a piezo electric sensor (PZT). Recently, Ferreira et al. [4] validated the technique using a plate with known vibrational behavior and proposed improvements, as the usage of a microphone to get better coherence between the results.

In this work, the wing of the Anequim, which is a prototype airplane developed by the CEA (from Portuguese, Center for Aeronautical Studies) of the UFMG, was submitted to the modal analysis testing using acoustic excitation. The experimental modal parameters, natural frequencies and mode shapes, were compared with the theoretical modal parameters calculated using Finite Element Method.

2 Theory

2.1 Modal Analysis

For extracting modal parameters such as natural frequency, damping factor and vibration modes, we can use the Theoretical Modal Analysis and Experimental Modal Analysis [8]. The first procedure is the formulation of a mathematical model of the structure under study through a discretization technique, as the Finite Element Method (FEM). The second procedure uses the experimental data obtained from the system response, which are usually given by Frequency Response Function (FRF). In modal analysis technique, the FRF of the structure can be measured at a single point, with the impulsive excitation applied elsewhere in the structure, or by the principle of reciprocity, the structure can be excited at a single point, using random broadband signals, with the frequency response function measured at various points of the structure.

Ferreira et al. [4] used acoustic excitation to measure the natural frequencies and mode shapes of a carbon plate. They obtained results with less than 10% of difference when compared to the numerical model, and less than 5% compared to a modal analysis with impact excitation. In addition, they pointed some limitations of the technique, as the difficulty to excite the system below 10 Hz and low data coherence below 15 Hz.

There are several ways to treat the data obtained from the system FRF. For the experimental analysis, the method of Chebyshev Orthogonal Polynomials [9] was implemented in a Matlab® code. Further explanations of the method can be obtained from Arruda et al. [10].

2.2 Anequim Project

Anequim is a racer airplane 100% build with carbon fiber materials using computerized machine systems. It was designed and built at Center for Aeronautical Studies of Federal University of Minas Gerais (CEA –UFMG), using 3D design tools and supported by computational codes for aerodynamic design, structural and aero-elastic analysis. Anequim uses an aeronautical four-cylinder engine with displacement of 360 in^3 and achieves a project top-level speed of 575 km/h (310 kts). With this velocity, Anequim is the world's fastest four-cylinder airplane ever built and set five world in the FAI C1a category (maximum take-off weight under 300 kg). For average speed over 3 km with restricted altitude, Anequim reached 521.08 km/h (323.78 mph), beating the previous record of 466.83 km/h (290.07 mph). This velocity range brings the need of a detailed flutter analysis. Figure 1 shows the Anequim project.

To perform flutter analysis, Silva [11] developed a Finite Element Model (FEM) of Anequim wing using the software FEMAP®/NX NASTRAN®. The model used a mixed mesh, and it is composed of CQUAD4 elements, with LAMINATE formulation, to model the principal structural components (spar, ribs and panels). RBE2 rigid elements were used to model the aileron articulation line. MASS elements were used to model the fuel mass and properties of the

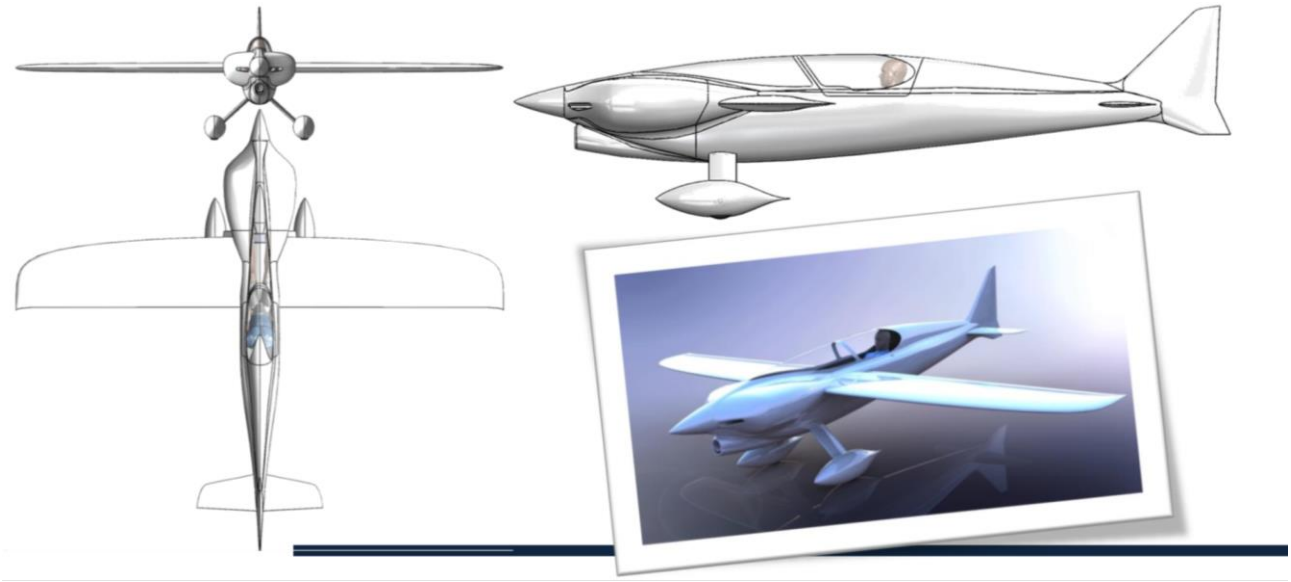

Fig. 1. Anequim project

airplane`s gravity center. RBE3 elements were used to transfer the mass weight to the structure. SPRING elements were used to model the aileron`s command stiffness. Figure 2 shows the model constructed by Silva [11].

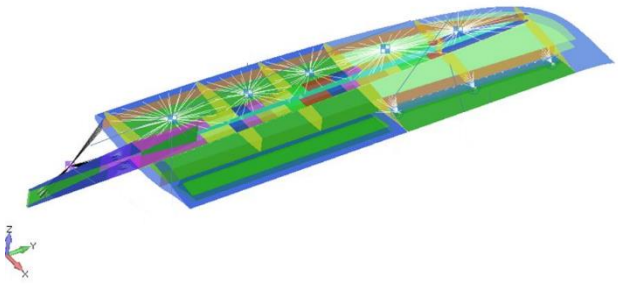

Fig. 2. Detail of the wing used into FEM. [11]

The frequencies obtained from this model (Tab. 1) were used comparison basis to the results of the GVT

Tab. 1. Wing numerical frequencies - Adapted from Silva (2014)

Mode	Frequency [Hz] (1)	Mode shape
1	19.6	First bending
2	37.81/36.48	Local Modes
3	0, 20 and 40(2)	Aileron rotation
4	62.3	Second Bending
5	69.7	First Torsion

(1) Modes with two frequencies correspond to Symmetric and Antisymmetric cases, respectively;
(2) Values of command stiffness were adjusted to obtain these results, according to aeronautical standards;

2.3 FRF Estimators

Noise is inevitable and is always present in an experimental measurement, so one must consider it in the results obtained. Analyzing Fig. 3, one can see that the frequency response function for the system in question, $H(\omega)$, is given by the relation between $X(\omega)$ and $F(\omega)$. However, it is not possible to measure the real values of $x(t)$ and $f(t)$ since they are contaminated by noise $n(t)$ and $m(t)$, respectively. Therefore, in experimental analyzes, we use estimators obtained from the noise data to characterize the system.

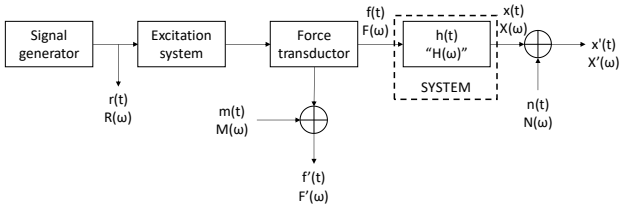

Fig. 3. Open mesh measurement system with external reference signal

According to Maia e Silva [12], the estimators $H_1(\omega)$, $H_2(\omega)$ and $H_3(\omega)$ are the most used in the practical analysis. They are defined from direct and crossed power spectra of the signals:

$$H_1(\omega) = \frac{S_{f'x'}(\omega)}{S_{f'f'}(\omega)} \quad (1)$$

$$H_2(\omega) = \frac{S_{x'x'}(\omega)}{S_{x'f'}(\omega)} \quad (2)$$

$$H_3(\omega) = \frac{S_{r'x'}(\omega)}{S_{r'f'}(\omega)} \quad (3)$$

Where $S_{f'x'}(\omega)$ is the cross spectrum between the input and output with noise, $S_{f'f'}(\omega)$ is the auto spectrum of the output with noise, $S_{x'x'}(\omega)$ is the auto spectrum of the input with noise, $S_{x'f'}(\omega)$ is the cross spectrum between the output and input with noise, $S_{r'x'}(\omega)$ is the cross spectrum between the reference signal and output with noise and $S_{r'f'}(\omega)$ is the cross spectrum between the reference signal and input with noise

Since $H_1(\omega)$ and $H_2(\omega)$ are based only on the signals of $x(t)$ and $f(t)$, they should provide the same result. Thus, the relationship between these two estimators defines a quality indicator of the analysis called ordinary coherence:

$$\frac{H_1(\omega)}{H_2(\omega)} = \frac{S_{f'x'}(\omega)}{S_{f'f'}(\omega)}\frac{S_{x'f'}(\omega)}{S_{x'x'}(\omega)} = \frac{S_{f'x'}(\omega)}{S_{f'f'}(\omega)}\frac{S_{f'x'}{}^*(\omega)}{S_{x'x'}(\omega)}$$

$$\gamma^2(\omega) = \frac{\left|S_{f'x'}(\omega)\right|^2}{S_{f'f'}(\omega)S_{x'x'}(\omega)}$$

where $\gamma^2(\omega)$ is the ordinary coherence of the system.

Coherence is a normalized coefficient of correlation between the measured force and the measured response signal at each frequency value. In practice, the coherence function is always greater than zero and less than one. According to Maia and Silva [12], coherence drops are caused by one or more of the following conditions

- The system that relates $f(t)$ e $x(t)$ is not linear;
- FRF estimators have systematic errors (polarization);
- External noise is present in FRF measurements;
- The measured response is due to other external excitations besides $f(t)$

3 Experimental setup for the modal analysis

All experiments were made at the airplane's left wing. The wing was removed from the airplane and fixed by two points to simulate cantilevered. The choice of the quantity and location of the measurement points was made considering the tradeoff between refinement of the results and experimental time. The mesh consists of 62 points, with refinement close to the aileron and wing tip, as shown in Fig. 3.

The wing was excited using a self-made 12 inches speaker and the response measured with a PCB 333A3 accelerometer in each one of the 62 points (Fig. 4). The vibration data-logger/analyzer used to record the signals was LDS PHOTON II. The data were analyzed using a Matlab® code with Chebycheff Orthogonal Polynomials method to extract the experimental natural frequencies and the mode shapes. The LDS PHOTON II was used to generate the excitation signal and send to the speaker. A PCB microphone was placed between the speaker and the wing to be used as the refence for the Frequency Response Functions (FRFs). The speaker was located under the wing around 200 mm. It is important to mention that the experiments showed that the best excitation was obtained with the speaker at the wing tip. The experimental setup is shown in Fig. 5.

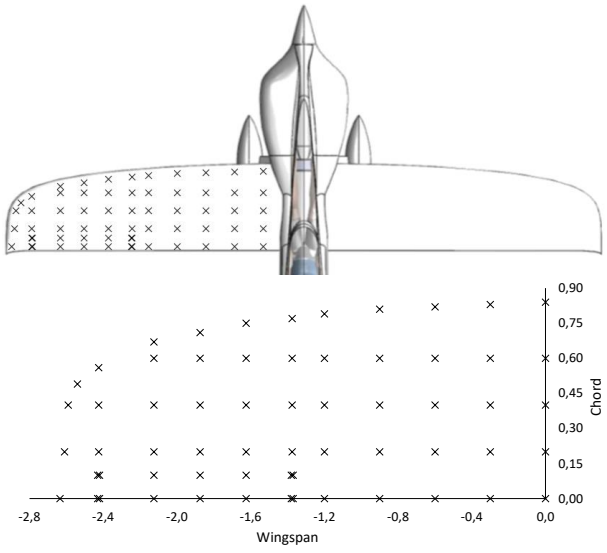

Fig. 4. Schematic diagram of the measurement points

According to Silva [11], the first five fundamental frequencies occurs below 90 Hz. Therefore, the excitation frequencies were generated using a Sweep Sine with variable amplitude and frequency from 5 Hz to 90 Hz in three seconds. The measurements were performed using a 240 Hz of sampling frequency with 0.16 Hz of discretization frequency using Hanning window. The system made 10 measurements and took the results average.

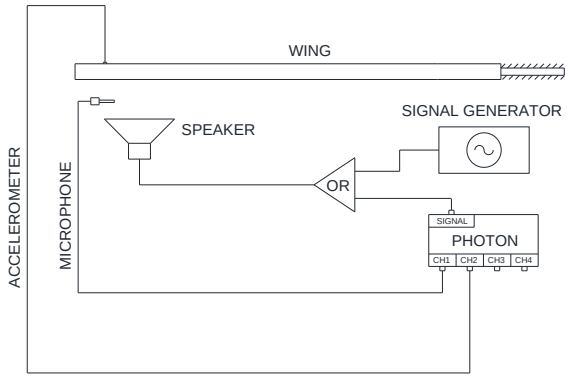

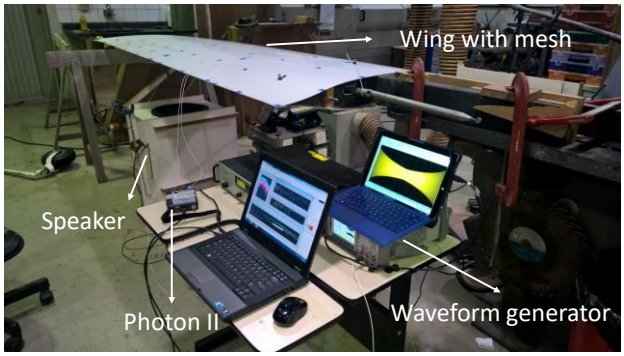

Fig. 5. Acoustic excitation experimental assembly

4 Results and Discussions

4.1 Natural frequencies and modal shapes

Fig. 6 shows the Frequency Response curves and coherence for the 62 measurement points. The region below 15 Hz presented problems like those reported by Ferreira et al. [4]. In this range, the data presented noise and coherence was below 1. The noise can be attributed to the speaker inability to excite the wing at low frequencies.

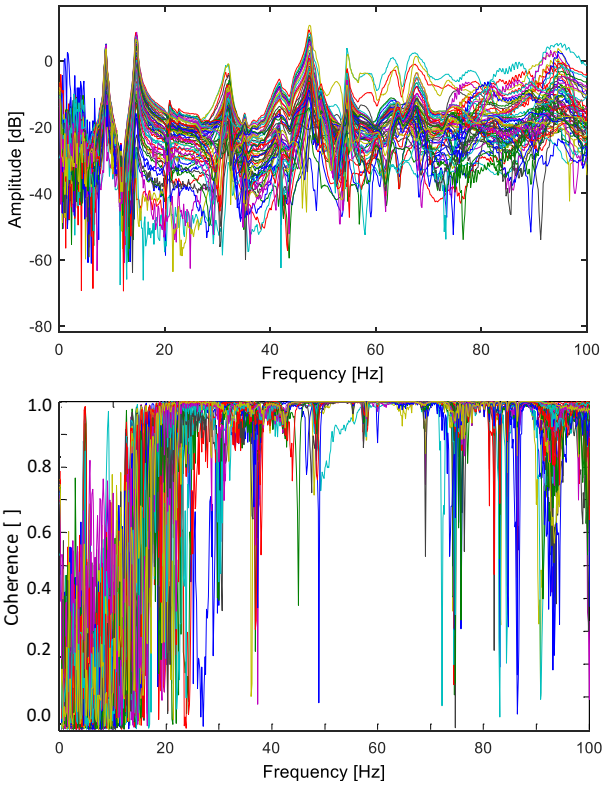

Fig. 6. FRF's and Coherence

Tests with the excitation system showed that the speaker can generate mechanical waves below 5 Hz, but the power transmitted at this frequency band is not sufficient to excite such a large object as the wing. Problems with coherence can also be attributed to the presence of ambient noise during the test. The usage of a microphone as reference reduced the problem of coherence drops at FRF peaks.

In the frequency range between 15Hz and 90Hz, the data presented low noise with some dispersion after 80 Hz. Tab. 2 present the identified modes compared with the results obtained by Silva [11].

Among the identified frequencies, there are elastic modes of the structure and modes produced by the interaction with the support. However rigid the experimental coupling and the support used, they will never have infinite stiffness as the constraint applied in finite element analysis. This phenomenon causes the appearance of the modes of interaction mentioned. In this work will be presented only the modal forms of the elastic modes, except for the first rigid body mode caused by the deformation of the crimp at 8.90 Hz

Tab. 2. Comparison between experimental and numerical frequencies from 15 Hz to 90 Hz

Mode	Numerical Frequency [Hz]	Experimental Frequency [Hz]	Mode
1	-	8.90	Rigid Body
2	19.6	14.7	First bendig
3	62.3	41.7	Second Bending
4	69.7	49.4	Torsion

The natural frequencies obtained for all modes were lower than the numerical ones. This may be related to problems in the crimping, mass differences between the model and the simulation and differences in material properties. Finite element models usually overestimate the system stiffness. The adjustment of the numerical model is beyond the scope of this work and will be left as suggestions for future work. As an example of a mode caused by the boundary condition, Fig. 7 presents the mode of rotation about the support.

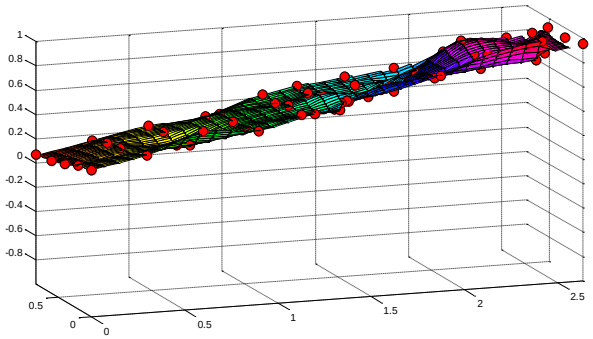

Fig. 7. Rigid body mode. Experimental Frequency = 8.90 Hz

Figures 8 to 10 show the comparison between numerical and experimentally identified modes. Figs. 8, 9 and 10 show that the modal shapes obtained experimentally approximated those predicted by the numerical model. This fact attests the ability of the method to excite and obtain the natural frequencies and modal forms of larger and more complex structures.

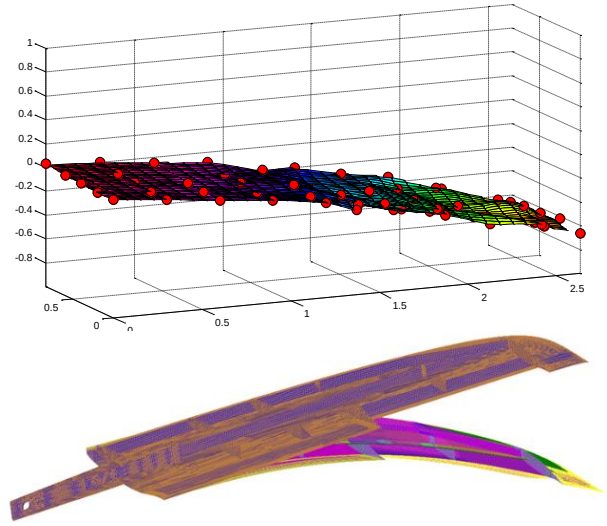

Fig. 8. First bending mode: (a) Experimental frequency = 14.7 Hz; (b) Numerical frequency = 19.6 Hz

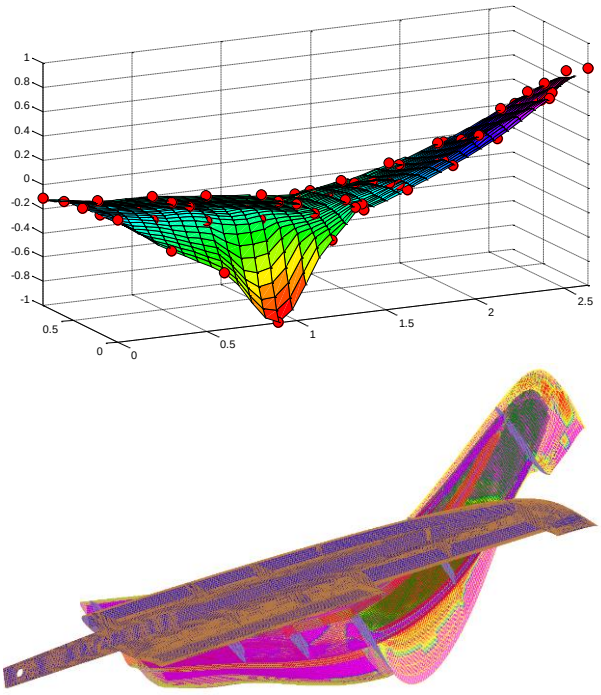

Fig. 9. Second bending mode: (a) Experimental frequency = 41.7 Hz; (b) Numerical frequency = 62.3 Hz

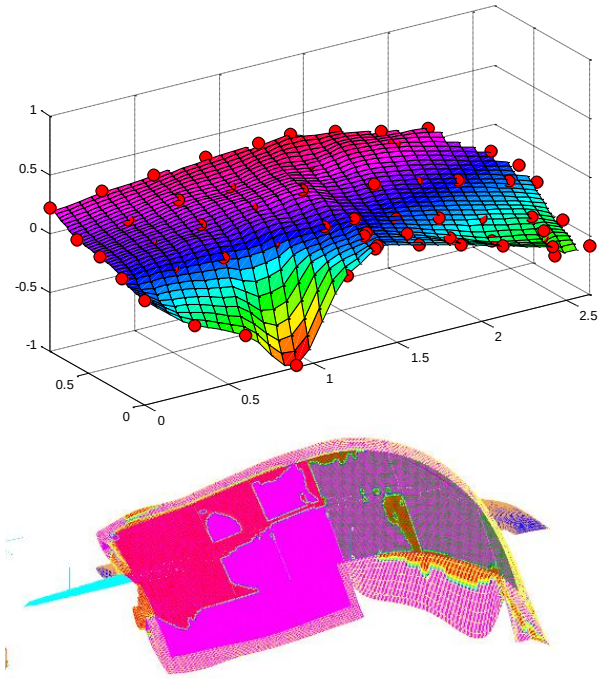

Fig. 10. First torsion mode: (a) Experimental frequency = 49.4 Hz; (b) Numerical frequency = 69.7 Hz

The mesh used for the tests proved to be sensitive enough to measure even local modes at the trailing edge, as shown in Figs. 7 and 8. This deflection occurs due to the low stiffness of the trailing edge when compared to the rest of the structure

To separate the elastic and rigid body modes, the stiffness of the support was changed. This leads to a significant change in the values of natural frequency for the rigid body modes, while the elastic modes do not change or have few variations. Fig. 11 shows this variation between two tests.

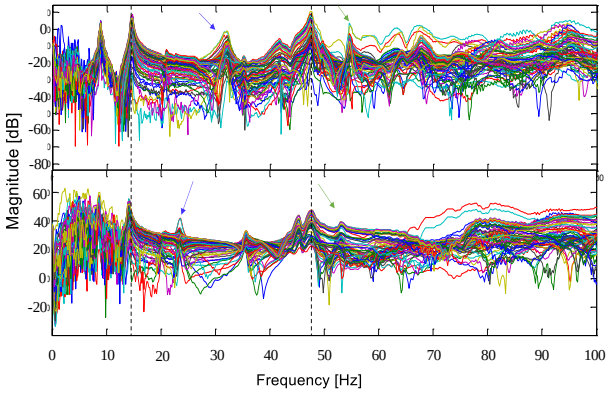

Fig. 11. Comparison of the Frequency Response Function of two tests with different bearing rigidity. Upper: greater stiffness in support; Low: less stiffness in support

It is possible to notice that some modes did not have their frequency changed, as in the case of the modes in 14.7 Hz and 47.5 Hz. These are indicated by dashed lines. The modes indicated by arrows had their natural frequency value changed between one test and another, but they modal form did not change, which characterizes modes of interaction with the support.

Silva [11] predicted local modes at 37.8 Hz and aileron modes at 0 Hz (Rigid body), 20 Hz and 40 Hz. Both modes were not observed in the present analysis. Local modes are hard to detect in a global analysis, as they require local measurements or a refined mesh. Silva obtained aileron modes according to aeronautical standards and are they only theoretical. The aileron command stiffness was not changed during the experiment, so these modes could not be observed at this study.

4.2 Microphone Distance Sensitivity

Variations in the relative position of the microphone may lead to different pressure measurements due to loss of acoustic wave energy during propagation. To evaluate these variations, tests with different configurations were performed.

In these tests, the distance between the sound box and the wing, as well as the amplitude of the excitation wave, were kept fixed. The distance between the microphone and the wing was varied, having as a control the microphone at 10 mm of it. Then, the estimator H_1 was calculated for the same one point of the structure at each relative distance. Fig. 12 presents these estimators and the data coherence for each assay.

The H_1 estimators decrease in magnitude by increasing the relative distance, that is, by moving the microphone away from the wing and approaching it from the loudspeaker. A reduction in the distance between the microphone and the cone increases the value of the measured pressure and, consequently, the value of the auto-spectrum of the signal. As the H_1 estimator is calculated by a ratio between the cross-spectrum and the input self-spectrum, an increase in the denominator reduces the magnitude of the estimator.

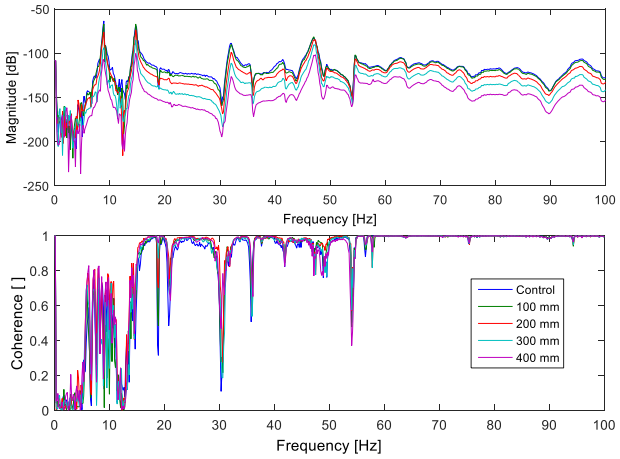

Fig. 12. FRF Estimator H_1 (a) and coherence (b) for the sensitivity test of the microphone position

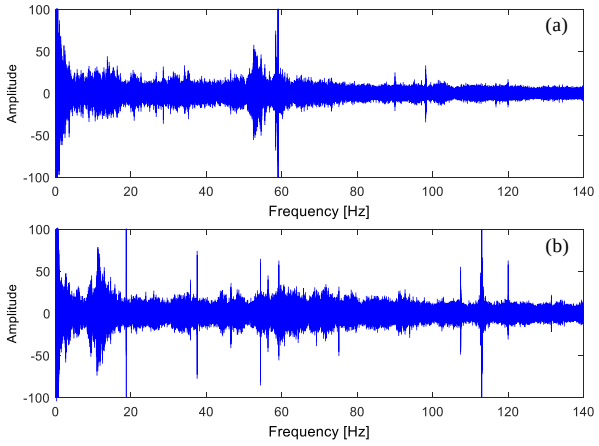

Fig. 13. Ambient noise where the tests were performed: (a) at dawn and (b) during the day

The coherence of the data practically does not change with the distance. This is because the phase change between the wave picked up by the microphone and the one that reaches the wing is negligible. Considering excitations between 5 Hz and 150 Hz, we have wavelengths of 68.0 m and 2.27 m, respectively. These wavelength values are greater than the longer distance tested.

For the tests, a fixed distance equal to 10 mm between the wing and the microphone was adopted to avoid compatibility problems between FRF's.

4.3 External noise

As a method via acoustic excitation, the result of the tests is influenced by ambient noise. This occurs mainly in regions of low frequency where the signal/noise ratio is lower. To characterize the influence of noise on FRF, measurements were taken at the CEA (Center for Aeronautical Studies) where the tests were performed both during the day, with people working and machines in operation, and at dawn when the ambient noise is lower. Fig. 12 shows the frequency spectrum picked up by the microphone for both conditions.

One may notice an increase in peak frequency in the spectrum captured during the day. Spikes in a narrow frequency range are assigned to structures or machines that generate well-defined disturbances, such as motors or pneumatic tools. In these, the frequency of rotation or oscillation is practically constant, which leads to narrow peaks in the spectrum. As an example, the numerical cutting machine present in the workshop operates at 8000 RPM or 133.3 Hz. This value can be observed in the frequency spectrum as the last peak indicated to the right.

In addition, an increase in the region between 50 and 120 Hz can be observed, which explains in part the noise observed in FRF's. However, in this region the signal/noise ratio is high, which reduces the influence of noise. The evaluation of the influence of noise according to the region can be done by observing Fig. 13. Here we have the noise spectrum (a), two FRF's (b) and the respective coherences (c). The functions were chosen to portray the influence of noise on points of different signal-to-noise ratios. Point 3 is located at the root of the wing, 400 mm from the trailing edge. In addition, it is close to the wing spar, which leads it to have few displacements. Point 53 is located on the same line along the chord, but at the tip of the wing, which leads to large displacements, especially in flexion or torsion modes.

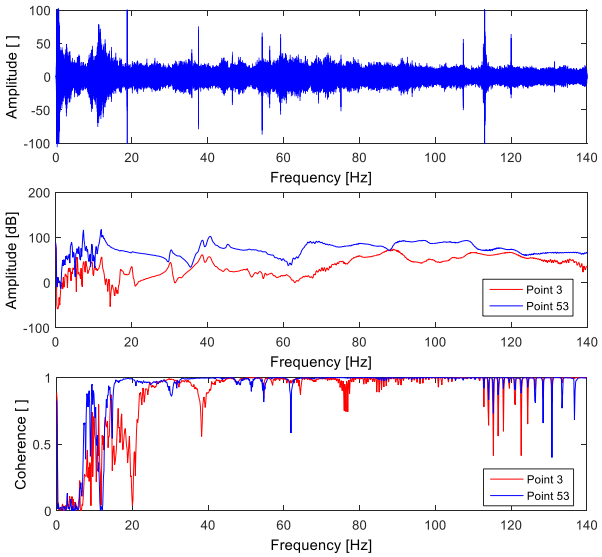

Fig. 14. Evaluation of the influence of ambient noise: (a) Noise spectrum, (b) FRF estimators and (c) Coherence

Observing Figs. 14 (b) and (c), although both points have an abrupt coherence drop near 12 Hz, point 3 is more influenced by the presence of low frequency noise. The decrease in 12 Hz is caused by an increase in noise in this value, as can be seen in Fig. 14 (a). However, after this drop the coherence of point 53 returns to values close to 1 and remains in this range, except for some falls in peaks of antiresonance. Point 3 has low coherence up to 20 Hz and still has a drop in some noisy frequencies, such as 18 Hz, 38 Hz and 75 Hz. This shows how much a low displacement point is subject to noise interference.

For this test, low-frequency vibrations are the most difficult to treat because, in addition to being inaudible, they are usually caused by large structures that either are part of the environment or are difficult to move. Vibrations of higher frequencies, in addition to being audible, are often attached to machines or people, which can be turned off or minimized. Noise in an experiment with acoustic excitation is difficult to eliminate, especially when performed in an environment such as a workshop or hangar. However, the method proved to be robust enough to identify vibration modes even with active noises. In view of the application of the technique, this robust character is essential, since the movement of an aircraft or a large structure to a different location for testing purposes is impracticable. As a suggestion for noise reduction, the test can be performed outside working hours, such as night or dawn. This would avoid displacement of the structure and minimize noise caused by machines and processes near the test site.

4.4 Evaluation of FRF estimators influence

According to Maia e Silva [12], the estimators H_1, H_2 and H_3 are the most used in the practical analysis. Also, the H_3 estimator is the one that suffers the least influence of external noises.

The Photon II acquisition system allows recording of data in time domain for the subsequent treatment and calculation of the desired estimator or the analysis in the frequency domain with the real-time calculation of the H_1 or H_2estimators.

For the evaluation of the influence of the estimators on the results, data were recorded in time domain and the estimators were calculated from it. In this comparison, an acquisition frequency of 375 Hz was used and data were recorded for 120 seconds at each measurement point. For the frequency domain treatment, a block size of 2000 points and the Hanning window were used. Fig. 15 shows the mean of the estimators in the frequency domain calculated with the 62 measurements.

It can be noted that the three estimators behaved similarly in the central region of the frequency range, differing mainly in the extremities. The H_1 and H_3 estimators present less noise at low frequencies when compared with the H_2 estimator. In addition, they remain very close throughout the frequency range, except for the region below 5 Hz.

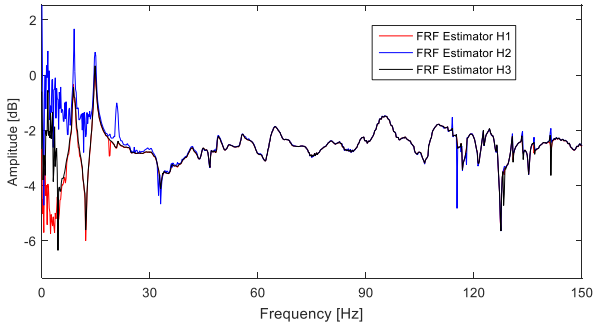

Fig. 15. Comparison between estimators H_1, H_2 e H_3

5 Conclusion

The experiment showed that acoustic excitation is a feasible technique in the studied frequency range. This approach aims to facilitate Groung Vibration Testing (GVT) and cause less interference of electromechanical shakers in the structure.

The technique was able to identify both the overall modes of the structure and the rigid body modes. Because it is a more complex structure, it also has local modes that were identified mainly in the trailing edge region, due to their lower stiffness.

The influence of microphone distance, ambient noise and different frequency response function (FRF) estimators were also analyzed.

The results obtained attest to the ability of the technique to excite and to identify modes of vibrations of complex structures. They also prove the robustness of the method to the influence of external noise, since the tests were carried out in a typical place of construction and storage of aircraft. This is desirable because the movement of an aircraft to a place of low ambient noise, such as an anechoic chamber, is logistically complicated.

However, more studies are needed to determine the source of the problem with the coherence below 15 Hz. As a suggestion for future works would be to use a focused excitation in this frequency with a bigger speaker or a different type of signal. Another suggestion is to measure the acceleration of both wings to determine asymmetric and antisymmetric configurations.

6 References

[1] Scanian, R.H., Rosenbaum, R. *Aircraft vibration and flutter*; 1996.

[2] Allen, B., Harris, C., Lange, D., *An inertially referenced noncontact sensor for ground vibration tests.* Sound and Vibration, January 2010.

[3] Daborn, P.M., Ind, P.R., Ewins, D.J., *Enhanced ground-based vibration testing for aerodynamic environments*, Mechanical Systems and Signal Processing, Volume 49, Issues 1–2, 20 December 2014, Pages 165-180.

[4] Ferreira, L. P. S., Donadon, L. V., Iscold, P. H, Ribeiro, G. M., *Modal analysis via acoustic excitation – Application on a carbon plate*. In Proccedings of the International Symposium on Solids Mechanics – MecSol 2015. Belo Horizonte, Brasil

[5] Collini, L., Garziera, R., Mangiavacca, F., *Development, experimental validation and tuning of a contact-less technique for the health monitoring of antique frescoes*, NDT & E International, Volume 44, Issue 2, March 2011, Pages 152-157.

[6] Assmus, M., Jack, S., Weiss, K.-A. and Koehl, M. (2011), *Measurement and simulation of vibrations of PV-modules induced by dynamic mechanical loads*. Prog. Photovolt: Res. Appl., 19: 688–694.

[7] Zhang, M.M., Katz, J., Prosperetti, A., *Enhancement of channel wall vibration due to acoustic excitation of an internal bubbly flow*, Journal of Fluids and Structures, Volume 26, Issue 6, August 2010, Pages 994-1017

[8] Souza, F.S., *Análise modal em materiais compósitos com adição de nanoparticulas*. Term paper, Universidade Federal de Minas Gerais, Belo Horizonte, 2008

[9] Mason, J.C., Handscomb, D., *Chebyshev Polynomials*. Chaoman & Hall/CRC, 2003

[10] Arruda, J. R. F. ; Rio, S. A. V. ; Santos, L. A. S. B. . *A space-frequency data compression method for spatially dense laser Doppler vibrometer measurements*. Shock and Vibration, New York, NY, v. 3, n. 2, p. 127-133, 1996.

[11] Silva, G. S, *Análise De Flutter da Aeronave CEA 311 Anequim*. Term paper, Universidade Federal de Minas Gerais, Belo Horizonte, 2014

[12] Maia, N. M. M., Silva, J. M. M., *Theoretical and Experimental Modal Analysis*, Hertfordshire, Research Studies Press, 1997

7 Contact Author Email Address

mailto:leonardopsf@ufmg.br

Copyright Statement